A Novel Approach for Miniaturization of Slot Antennas

Reza Azadegan, *Student Member, IEEE,* and Kamal Sarabandi, *Fellow, IEEE*

***Abstract*—With the virtual enforcement of the required boundary condition (BC) at the end of a slot antenna, the area occupied by the resonant antenna can be reduced. To achieve the required virtual BC, the two short circuits at the end of the resonant slot are replaced by some reactive BC, including inductive or capacitive loadings. The application of these loads is shown to reduce the size of the resonant slot antenna for a given resonant frequency without imposing any stringent condition on the impedance matching of the antenna. In this paper, a procedure for designing this class of slot antennas for any arbitrary size is presented. The procedure is based on an equivalent circuit model for the antenna and its feed structure. The corresponding equivalent circuit parameters are extracted using a full-wave forward model in conjunction with a genetic algorithm optimizer. These parameters are employed to find a proper matching network so that a perfect match to a 50 Ω line is obtained. For a prototype slot antenna with approximate dimensions of $0.05\lambda_0 \times 0.05\lambda_0$ the impedance match is obtained, with a fairly high gain of -3 dBi, for a very small ground plane ($\approx 0.20\lambda_0$). Since there are neither polarization nor mismatch losses, the antenna efficiency is limited only by the dielectric and Ohmic losses.**

***Index Terms*—Miniaturized antenna, slot antenna.**

I. Introduction

THE TOPIC of small antennas has been a subject of interest for more than half a century, but in recent years, it has attained significant attention because of an exorbitant demand for mobile wireless communication systems. The need for antenna miniaturization stems from the fact that most mobile platforms have a limited space for all of the required antennas in ever increasing wireless systems. Compact antennas are needed so that more antennas can be closely packed together without the risk of mutual and parasitic coupling between them. For local area networks, there is an emerging interest in making antennas small enough to ultimately fit on a single chip with the rest of the receiving front-end. As part of a general trend in monolithic circuit integration, using the area of substrate more efficiently is another strong motivation. At low frequencies (HF–VHF), miniature antennas are in high demand, since the antenna size often imposes a significant limitation on the overall size of a portable wireless system.

Earlier studies on small antennas focused on establishing a relation between the volume occupied by the antenna to radiation characteristics and the bandwidth of the antenna [1]–[4]. In these studies, a relation between the Quality Factor (Q) of the antenna and the radius of the smallest fictitious spherical enclosure containing the antenna was derived. This derivation was based on the spherical wave function expansion of the fields radiated from the antenna. Each spherical mode was represented by an equivalent circuit for which a quality factor (Q_n) was calculated. Since the spherical eigenfunctions are orthogonal, no energy could be coupled among modes. Therefore, the Q of the antenna was expressed as a function of the Q of individual modes. Finally, it was shown that the quality factor of the lowest order mode is a lower bound for the Q of a single resonant antenna [2]. A similar approach was adopted by Collin [5] for cylindrical antennas using cylindrical wave functions to provide a tighter lower limit on the Q of thin antennas with large aspect ratios. Results of these studies have been summarized and referred to as the fundamental limitations of small antennas [6]. However, in the aforementioned papers there are no discussions about procedures to design miniaturized antennas.

In addition to high Q, a direct result of antenna miniaturization is reduction in the antenna efficiency owing to the relatively high conduction and/or polarization currents on the conductors or within the dielectric part of the antenna structure. Furthermore, the matching network of a miniaturized antenna is usually complex and lossy. An example of miniaturized antennas is a meandered antenna where a half wavelength dipole is made compact by meandering the wire [7]. A similar approach can be applied to design a meander type slot antenna [8]. In order to increase the efficiency of these antennas by reducing dissipation, the use of a high temperature superconductor (HTS) has been proposed [9], [10]. On the other hand, meandered antennas are very hard to match to a 50-Ω line. This difficulty is due to the fact that the radiation of almost in-phase electric currents flowing in opposite directions on closely spaced wires tend to cancel each other in the far-field region. This cancellation renders a considerable portion of opposing currents ineffective as far as radiation efficiency is concerned and leads to a very low radiation resistance that might have been increased using a two-strip meandered line [11]. Consequently, these antennas are difficult to match, and yet require a very low temperature of operation to control material losses [12].

Another approach for antenna miniaturization, reported in the literature, is to use very high dielectric constant materials in dielectric loaded antennas [13], [14]. Obviously, dielectric loading provides a size reduction factor on the order of $\sqrt{\varepsilon_r}$ for the leaky dielectric and cavity resonator type antennas (e.g., microstrip patch antennas), where ε_r is the relative permittivity of the dielectric material. This miniaturization method, however, is less effective for terminated transmission line antennas, such as slot or printed dipole antennas since these antennas see an effective permittivity (ε_{eff}), which is considerably less than ε_r.

Manuscript received August 24, 2001; revised February 18, 2002.

The authors are with the Radiation Laboratory, Department of Electrical Engineering and Computer Science, The University of Michigan, Ann Arbor, MI 48109 USA.

Digital Object Identifier 10.1109/TAP.2003.809853

Although this method of miniaturization is susceptible to surface wave excitation, it might be found beneficial, especially when the electrical thickness of the substrate is small compared to the wavelength. It is worth mentioning that this type of antenna miniaturization is not immune to the aforementioned adverse effects such as high Q, low efficiency, and complexity in the matching network.

Nevertheless, there is another important methodology in antenna miniaturization; that is, modifying the antenna geometry. Recently a new topology based on an S-shape quarter wavelength resonant slot antenna was reported by the authors [15]. A miniaturized quarter wavelength slot antenna was proposed using a short circuit at one end of the slot and an open circuit at the other end. The open circuit was realized by a coiled quarter wavelength slot-line. Using this design, a very efficient miniaturized antenna with dimensions of the order of $0.12\lambda_0 \times 0.12\lambda_0$ on a substrate having $\varepsilon_r = 4.0$ was constructed using a microstrip feed.

In this paper, we propose a novel procedure to design a miniaturized slot antenna where its dimensions (relative to wavelength) can be arbitrarily chosen, depending on the application, without any adverse effects on the impedance matching. As will be shown, in order to fine-tune the resonant frequency of this structure, the antenna is first fed by a two-port microstrip line, and then the location of the null in the insertion loss (S_{21}) is found and adjusted. To specify the terminating impedance at the second port in such a way that a perfect match is achieved, an equivalent circuit for the antenna is proposed and its parameters are extracted using a genetic algorithm (GA) in conjunction with a full-wave simulation tool. Finally, a prototype antenna is designed, fabricated, and its performance is evaluated experimentally.

II. Antenna Geometry

For a resonant slot antenna, one needs to apply two boundary conditions (BCs) at both ends of a slot line to form a resonant standing wave pattern. These two conditions are chosen so as to enforce zero electric current (open circuit) for a wire antenna or zero voltage (short circuit) for the slot antenna, and yield a half-wave resonant antenna. On the other hand, these alternative BCs result in a smaller resonant length than a half wavelength antenna [16]. One choice which is conducive to antenna miniaturization is the combination of a short circuit and an open circuit, which allows a shorter resonant length of $\lambda/4$ [15]. The choice of the two BCs, however, is not restricted to the above conditions, whereas the effect of reactive BCs in reducing the resonant length and antenna miniaturization is investigated in what follows.

A. Slot Radiator Topology

Starting from a $\lambda_s/2$ slot and in the view of the transmission line approximation for the slot dipole, the equivalent magnetic current distribution along a linear slot antenna can be expressed as

$$M(z) = M_0 \cos\left(\frac{\pi}{\lambda_s} z\right) \tag{1}$$

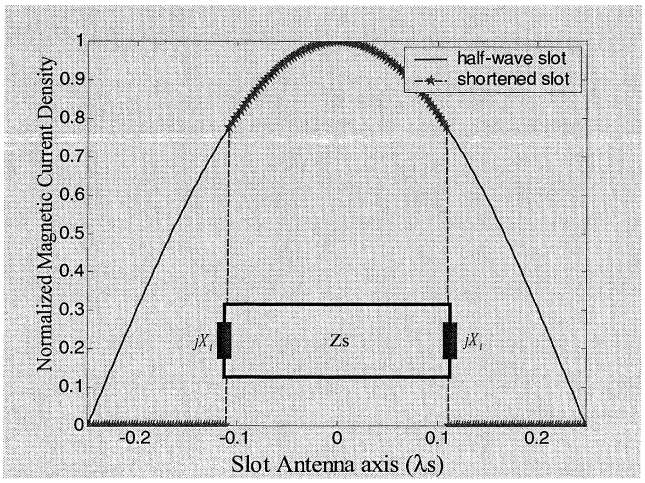

Fig. 1. Magnetic current distribution on a half wavelength and inductively terminated miniaturized slot antenna.

where λ_s is the guided wavelength in the slot-line. In (1), M_0 represents the amplitude of the magnetic current density (electric field across the slotline). This approximate form of the current distribution satisfies the short circuit BCs at the end of the slot antenna. If by using an appropriate boundary condition, the magnetic current density at any arbitrary point $|z'| < \lambda_s/4$ along the length of a modified slot antenna can be maintained the same as the $\lambda_s/2$ slot antenna, then it is possible to make a smaller slot antenna. Any size reduction of interest can be achieved so long as the appropriate BCs are in place at the proper location on the slot. Fig. 1 illustrates the idea where it is shown that by imposing a finite voltage at both ends of a slot, the desired magnetic current distribution on a short slot antenna can be established.

To create a voltage discontinuity, one can use a series inductive element at the end of the slot antenna. It should be pointed out that terminating the slot antenna with a lumped inductance or capacitance is not practical since the slot is embedded in a ground plane, which can in fact short-circuit any termination. To circumvent this problem, a lumped inductor could be physically realized by a compact short-circuited slotted spiral. To ensure inductive loading, the length of the spiral slot must be less than a quarter wavelength. Instead of a single inductive element at each end, it is preferred to use two inductive slotlines opposite of each other [see Figs. 2(c) and 3]. Since these two inductors in the slot configuration are in series, a shorter slotline provides the required inductive load at the end of the slot antenna. Another reason for choosing this configuration is that the magnetic currents flowing in opposite directions cancel each other's fields on the planes of symmetry, and thereby, minimize the near-field coupling effect of the inductive loads on the desired current distribution along the radiating slot.

It should be noted that the mutual coupling within the spiral slotline reduces the effective inductance, and therefore, a longer spiral length compared with a straight section [Fig. 2(c)] is needed to achieve the desired inductance. To alleviate this adverse effect, a narrower slot width must be chosen for the spiral slotline.

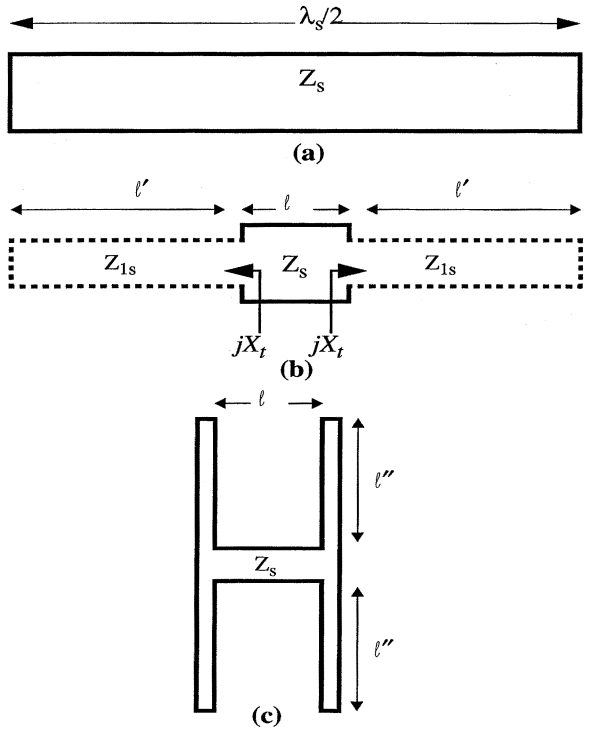

Fig. 2. Transmission line model of a slot antenna (a) half-wave slot antenna. (b) Inductively terminated slot antenna. (c) Two series inductive terminations.

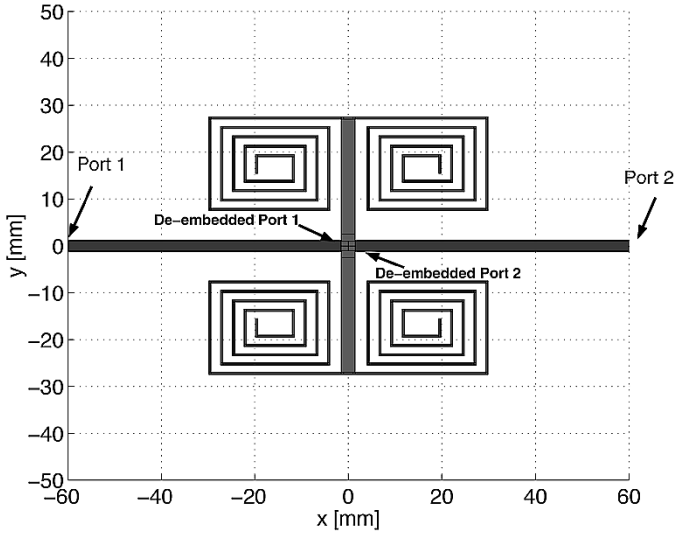

Fig. 3. Proposed antenna geometry fed by a two-port microstrip feed. This two-port geometry is used to find out the exact resonant frequency of the inductively loaded slot.

B. Antenna Feed

A microstrip transmission line is used to feed this antenna. The choice of the microstrip feed, as opposed to a coaxial line, is based on the ease of fabrication and stability. This feed structure is also more amenable to tuning by providing the designer with an additional parameter. Instead of short-circuiting the microstrip line over the slot, an open-ended microstrip line with an appropriate length extending beyond the microstrip-slot crossing point (additional parameter) can be used.

A coplanar waveguide (CPW) can also be used to feed the antenna providing the ease of fabrication, whereas it is more difficult to tune. Usually, a metallic bridge is needed to suppress the odd mode in the CPW. The use of CPW lines also reduces the effective aperture of the slot antenna, especially when a very small antenna is to be matched to a 50-Ω line. Typically for a low dielectric constant substrate, the center conductor in the CPW lines at 50 Ω is rather wide and the gap between the center conductor and the ground planes is relatively narrow. Hence, feeding the slot antenna from the center blocks a considerable portion of the miniaturized slot antenna [17]. There are other methods to feed the slot antenna with CPW lines, including an inductively or capacitively fed slot [18].

TABLE I
SLOTLINE CHARACTERISTICS FOR TWO DIFFERENT VALUES OF SLOT WIDTH w, AND THE DIELECTRIC CONSTANT OF $\varepsilon_r = 2.2$ AND THICKNESS OF $h = 0.787(mm)$ AND $f = 300$ MHz

$w(mm)$	$\lambda_s(mm)$	$Z_{0s}(\Omega)$
0.5	918	81
3.0	960	107

III. DESIGN PROCEDURE

In this section, a procedure for designing a novel miniaturized antenna with the topology discussed in the previous section is presented. To illustrate this procedure, a miniaturized slot antenna at 300 MHz is designed. This frequency is the lowest frequency at which we could accurately perform antenna measurements in the anechoic chamber, and yet, the miniature antenna is large enough so that standard printed circuit technology can be used in the fabrication of the antenna. A microwave substrate with a dielectric constant of $\varepsilon_r = 2.2$, a loss tangent of $\tan\delta \approx 10^{-3}$, and a thickness of 0.787 mm (31 mil) [19] is considered for the antenna prototype.

As the first step, the basic transmission line model is employed to design the antenna and then, a full-wave Moment Method analysis is used for fine tuning. Table I shows the finite ground plane slotline characteristic impedance Z_{0s} and guided wavelength λ_s for the above mentioned substrate and for two slot widths of $w = 0.5$ mm and $w = 3.0$ mm, all at 300 MHz. As mentioned before, the antenna size can be chosen as a design parameter, and in this example, we attempt to design a very small antenna with a length of $\ell = 55$ mm $\approx 0.05\lambda_0$. A slot width of $w = 3$ mm is chosen for the radiating section of the slot antenna. A slot antenna whose radiating slot segment is of a length ℓ, should be terminated by a reactance given by

$$X_t = Z_{0s} \tan \frac{2\pi}{\lambda_s} \ell' \tag{2}$$

in order to maintain the magnetic current distribution of a $\lambda_s/2$ resonant slot antenna (see Fig. 2). In (2)

$$\ell' = \frac{1}{2}\left(\frac{\lambda_s}{2} - \ell\right) \tag{3}$$

and Z_{0s} and λ_s are the characteristic impedance and the guided wavelength of the slotline, respectively. As mentioned before, the required terminating reactance of X_t can be constructed by two smaller series slotlines. Denoting the length of a terminating

slotline by ℓ'', as shown in Fig. 2(c), the relationship between the required reactance and ℓ'' is given by

$$\frac{X_t}{2} = Z'_{0s} \tan \frac{2\pi}{\lambda'_{0s}} \ell'' \tag{4}$$

where Z'_s and λ'_s are the characteristic impedance and the guided wavelength of the terminating slotline. A narrower slot is used to construct the terminating slotlines so that a more compact configuration can be achieved. As shown in Table I, the narrower slotline has a smaller characteristic impedance and guided wavelength which results in a slightly shorter length of the termination (ℓ''). Although ℓ'' is smaller than ℓ', the actual miniaturization is obtained by winding the terminating line into a compact spiral as seen in Fig. 3.

According to (2) and (4), and also the values for the guided wavelengths, ℓ'' is found to be $\ell'' = 193.7$ mm. Referring to Fig. 3, the vertical dimension (along the y axis) of the rectangular spiral should not exceed half of the length of the radiating slot segment (ℓ). This constraint on the inductive rectangular spiral is imposed so that the entire antenna structure can fit into a square area of 55 mm $\times$ 55 mm, which is about $0.05\lambda_0 \times 0.05\lambda_0$. Since the dielectric constant and the thickness of the substrate chosen for this design are very low ($\varepsilon_r = 2.2$), the guided wavelength ($\lambda_s = 96$ cm) is not very much different from that of free space ($\lambda_0 = 100$ cm). Thus, the miniaturization is mainly achieved by the proper choice of the antenna topology. It is worth mentioning that further size reduction can be obtained once a substrate with higher permittivity is used.

IV. Full-Wave Simulation and Tuning

In Section III, the transmission line model was employed for designing the proposed miniature antenna. Although this model is not very accurate, it provides the intuition necessary for designing the novel topology. The transmission line model ignores the coupling between the adjacent slot lines and the microstrip to slot transition. For calculation of the input impedance and exact determination of the length of different slotline segments, a full-wave simulation tool is required. IE3D, a commercially available Moment Method code is used for required numerical simulations [20].

Fig. 3 shows the proposed antenna geometry fed by a two-port 50 Ω microstrip line. The two-port structure is constructed to study the resonant frequency of the antenna as well as the transition between microstrip and the slot antenna. The microstrip line is extended well beyond the slot transition point so that the port terminals do not couple to the slot antenna. The radiating slot length is chosen to be $\ell = 55$ mm, and the length of the rectangular spirals are tuned such that the antenna resonates at 300 MHz. The resonance at the desired frequency is indicated by a deep null in the frequency response of S_{21}. The simulated S-parameters of this two-port structure are shown in Fig. 4. This figure indicates that the antenna resonates at around 304 MHz, which is close to the desired frequency of 300 MHz. In fact, the resonant frequency of the radiating structure must be chosen at a slightly higher or lower frequency. The reason is that small slot antennas have a low radiation conductance at the first resonance and therefore, it should be tuned slightly off-resonance if it is to be matched to a 50-Ω transmission line. Fig. 5 shows an

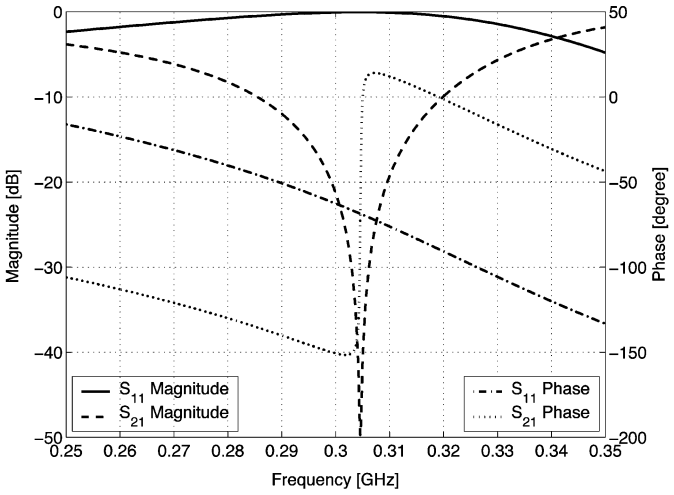

Fig. 4. S-parameters of the two-port antenna shown in Fig. 3.

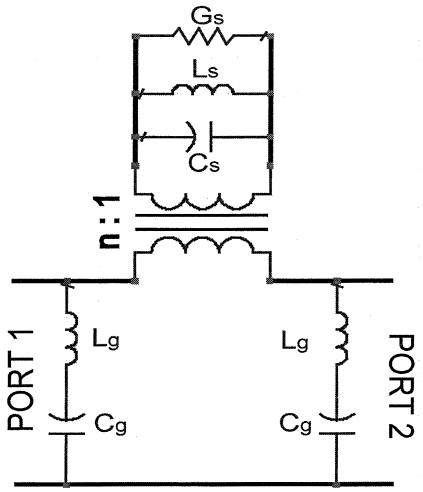

Fig. 5. Topology of the equivalent circuit for the two-port antenna.

equivalent circuit model for the two-port device when the transition between microstrip and slot line is represented by an ideal transformer with a frequency dependent turn ratio (n^2) [21], and the slot is modeled by a second order shunt resonant circuit near its resonance [22]. The radiation conductance G_s, which is also referred to as the slot conductance, attains a low value that corresponds to a very high input impedance at the resonant frequency. However, this impedance would decrease considerably, when the frequency moves off the resonance. The 4 MHz offset in the resonant frequency of the antenna is maintained for this purpose.

Having tuned the resonant frequency of the antenna, coupled to the two-port microstrip feed (Fig. 3), we need to design a lossless impedance matching network. This can be accomplished by providing a proper impedance to terminate the second port of the microstrip feed line. To fulfill these tasks systematically, we need to extract the equivalent circuit parameters shown in Fig. 5. It should be pointed out that for the proposed miniaturized slot antenna, a simplistic model for standard size slots, which treats the slot antenna as an impedance in series with the microstrip line is not sufficient. Essentially, the parasitic effects caused by the coupling between the microstrip feed and rectangular spirals

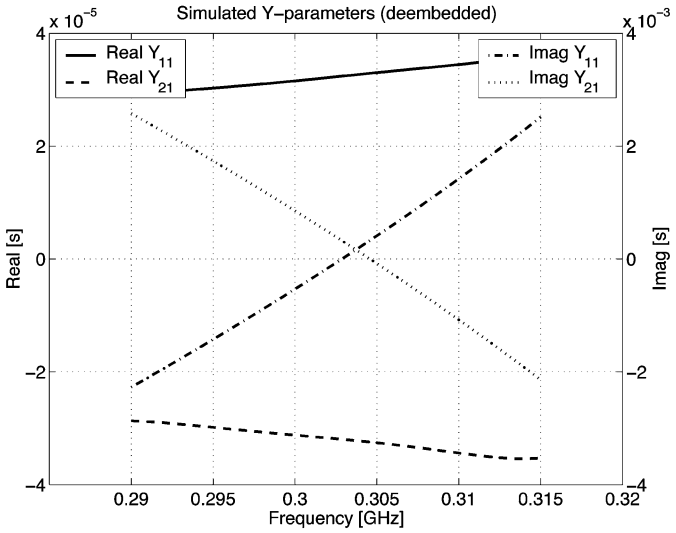

Fig. 6. Y-parameters of the two-port antenna after deembedding the microstrip feed lines.

as well as the mutual coupling between the radiator section and the rectangular spirals should also be included in the equivalent circuit.

A. Equivalent-Circuit Model

In this section, an equivalent circuit model for the proposed antenna is developed. This model is capable of predicting the slot radiation conductance and the antenna input impedance near resonance. This approach provides very helpful insight as to how this antenna and its feed network operate. As mentioned before, this model is also needed to find a proper matching network for the antenna.

Near resonant frequencies, the slot antenna can be modeled by a simple second order RLC circuit. Since the voltage across the slot excites the slot antenna at the feed point, it is appropriate to use the shunt resonant model for the radiating slot as shown in Fig. 5. The coupling between the microstrip and the slot is modeled by a series ideal transformer with a turn ratio n.

To model the feeding mechanism right at the cross junction of the microstrip and slot, it is necessary to deembed the effect of the microstrip lines between the terminals and the crossing points. There are different deembedding schemes reported in [24] and [25]. The advantage of proper deembedding, as opposed to the mere shifting of the reference planes by the corresponding phase factor is to exclude the effect of radiation and other parasitic effects of the line.

To model the parasitic coupling of the microstrip line and the slot (coupling of radiated field from the microstrip line and slot), two additional parasitic parameters, namely, L_g and C_g are included in the model. The use of shunt parasitic parameters has previously been suggested to model the effects of fields as perturbed by a wide slot [23]. Fig. 6 shows the deembedded Y-parameters of the two-port microstrip-fed slot antenna where the location of deembedded ports are shown in Fig. 3. Note that these two ports are now defined at the microstrip-slot junction.

TABLE II
THE PARAMETERS OF THE GENETIC ALGORITHM OPTIMIZER

Population Size	300
Number of Iteration	50,000
Chromosome Length	128
$P_{Crossover}$	0.55
$P_{Mutation}$	0.005

TABLE III
THE EQUIVALENT CIRCUIT PARAMETERS OF THE MICROSTRIP FED SLOT ANTENNA

Turn Ratio (n)	0.948007
$R_s(\Omega)$	33979
$L_s(\mu H)$	0.0207
$C_s(pF)$	13.1744
$L_g(\mu H)$	0.49997
$C_g(pF)$	0.125

According to the lumped element model of Fig. 5, the Y-parameters are given by

$$Y_{11} = \frac{-j}{L_g\omega - \frac{1}{C_g\omega}} + \frac{1}{n^2}\left[G_s + j\left(C_s\omega - \frac{1}{L_s\omega}\right)\right] \quad (5)$$

$$Y_{21} = -\frac{1}{n^2}\left[G_s + j\left(C_s\omega - \frac{1}{L_s\omega}\right)\right]. \quad (6)$$

Using reciprocity and noting the symmetry of the equivalent circuit, it can easily be shown that $Y_{11} = Y_{22}$ and $Y_{21} = Y_{12}$.

In order to extract the equivalent circuit parameters, a GA optimization code has been developed and implemented [26]. The sum of the squares of relative error for real and imaginary parts of Y-parameters over 40 frequency points around the resonance is used as the objective (fitness) function of the optimization problem. We ran the program with different random number seeds to ensure the best result over the entire domain of the parameters space. Also, the parameters were constrained only to physical values in the region of interest. The parameters of the GA optimizer are shown in Table II. Table III shows the extracted equivalent circuit parameters after 50,000 iterations.

The S-parameters of the equivalent circuit as well as the S-parameters extracted from the full-wave analysis are shown in Fig. 7. Excellent agreement is observed between the full-wave results and those of the equivalent circuit.

B. Antenna Matching

Having found the equivalent circuit parameters, the antenna's matching network can readily be designed. For matching networks, especially when efficiency is the main concern, lossless terminations are usually desired. Therefore, we seek a purely reactive admittance to terminate the feed line, which in fact is the load for the second port of the two-port equivalent circuit model. The explicit expression for a termination admittance (Y_t) to be placed at the second terminal of the two-port model in order to match the impedance of the antenna is given by

$$Y_t = -Y_{11} + \frac{Y_{12}^2}{Y_{11} - Y_0}. \quad (7)$$

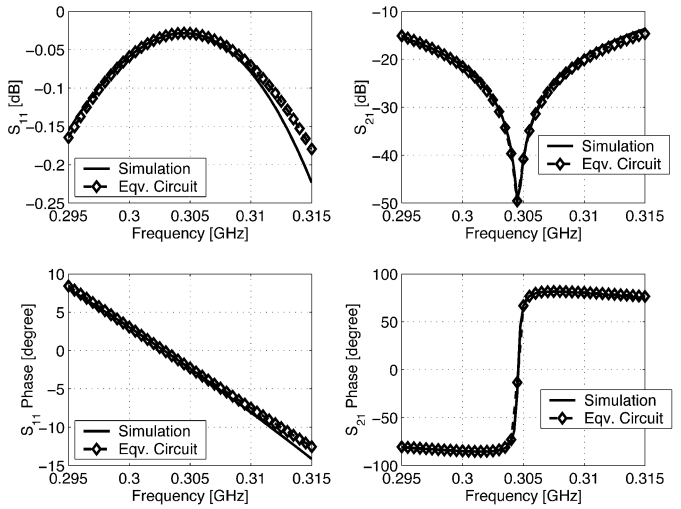

Fig. 7. Comparison between the full-wave simulated S-parameters of the antenna and that of the equivalent circuit.

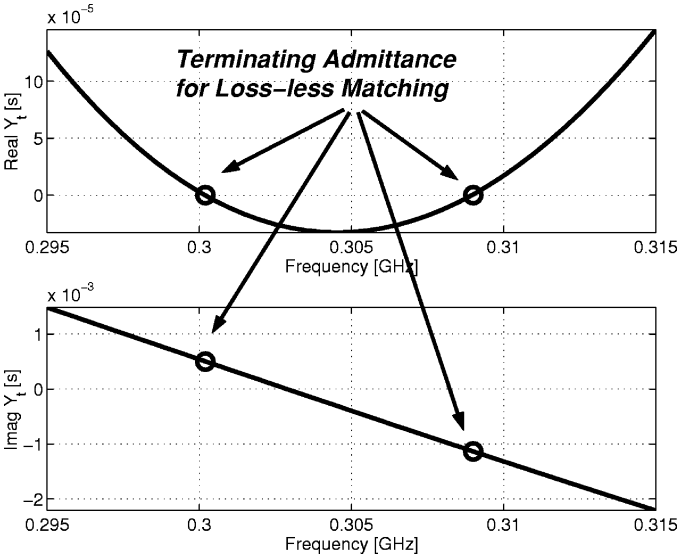

Fig. 8. The required terminating admittance for the second port of the two-port model in order to match the antenna to a 50-Ω line.

Fig. 8 shows the spectral behavior of Y_t for a standard 50-Ω line ($Y_0 = 0.02$ $\mho$). Interesting to note are the two distinct frequency points at which the real part of Y_t vanishes. This implies that we can match this antenna at these two frequency points, namely, 300 and 309 MHz. As mentioned earlier, a small slot antenna has a very low radiation conductance. The value of this low conductance, shown in Table III, suggests a very high input impedance of the order of 30 KΩ at resonance, considering the transformer turn ratio. Thus, in order to match the antenna to a lower impedance transmission line, the matching should be done at a frequency slightly off the resonance. At an off-resonance frequency, the input impedance does not remain a pure real quantity, however, the imaginary part can easily be compensated for by an additional reactive component created by an open-ended microstrip. At each resonance, there are two possibilities. One possibility is to match the antenna slightly below the slot resonance, that is 304 MHz (Fig. 4), and terminate the second port capacitively. The second possibility is to tune the antenna slightly above the slot resonance and terminate the second port inductively.

TABLE IV
THE PHYSICAL LENGTH OF THE 50-Ω MICROSTRIP LINE NEEDED FOR REALIZING THE TERMINATION SUSCEPTANCE, WHERE THE DIELECTRIC MATERIAL PROPERTIES ARE AS SPECIFIED IN TABLE I

$f\ (MHz)$	300	309
$Y_t(s)$	$j5.4 \times 10^{-4}$	$-j1.14 \times 10^{-3}$
$\lambda_g(mm)$	725.57	704.52
$Z_0(\Omega)$	50	50
Line extension (mm)	3.1514	345.80

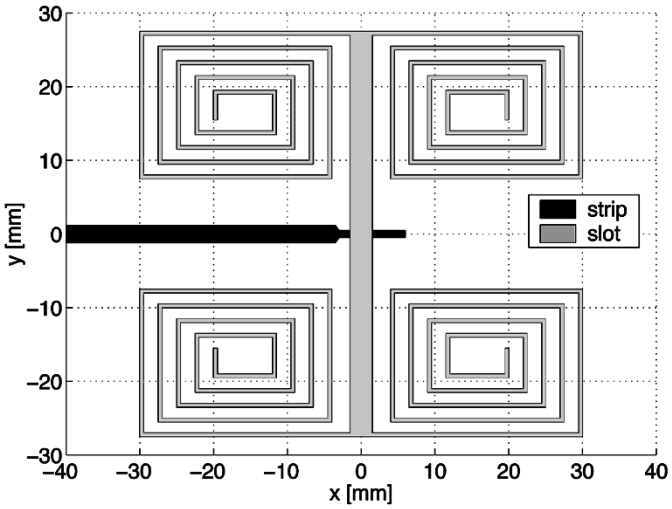

Fig. 9. The geometry of the antenna and its feed designed to operate at 300 MHz.

Based on what is shown in Table IV, a very short open-ended-microstrip line extension is required at the second port, in contrast with a quarter wavelength extension for an ordinary half wavelength slot antenna. This short extension introduces a small capacitance, which compensates the additional inductance introduced as a result of operating below resonance. After tuning the antenna, the original slot resonant frequency at 304 MHz, shifts down to the desired frequency of 300 MHz, as shown in Fig. 8 and Table IV.

V. ANTENNA SIMULATION AND MEASUREMENTS

In this section, simulation results for the proposed antenna are illustrated. Fig. 9 shows the antenna geometry matched to a 50-Ω line. As seen in this figure and suggested by Table IV, the feed line has been extended a short distance beyond the slot line. The width of the microstrip, where it crosses the slot, is reduced so that it may block a smaller portion of the radiating slot. It is worth mentioning that the effect of the feed linewidth on its coupling to the slot was investigated, and it was found that as long as the linewidth is much smaller than the radiating slot length, the equivalent circuit parameters do not change considerably.

As mentioned, the antenna has been simulated using a commercial software (IE3D) [20]. Using this software, the return loss (S_{11}) of the antenna is calculated and shown in Fig. 10. In

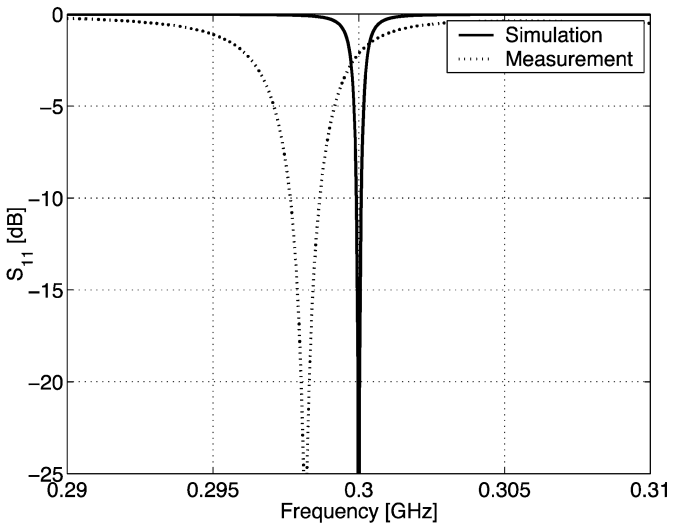

Fig. 10. Measured and simulated return loss of the miniaturized antenna.

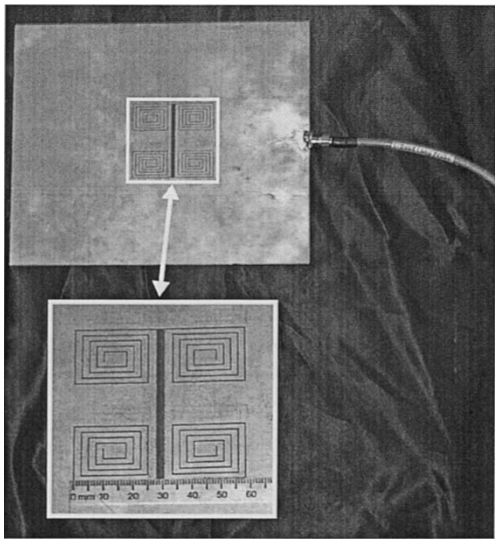

Fig. 11. A photograph of the fabricated antenna.

order to experimentally validate the design procedure, equivalent circuit model, and simulation results, the antenna was fabricated on a 0.787-mm-thick substrate with $\varepsilon_r = 2.2$ and $\tan\delta = 0.001$.

Fig. 11 shows a photograph of the fabricated antenna. The return loss (S_{11}) of the antenna was measured using a calibrated vector network analyzer and the result is shown in Fig. 10. The measured results show a slight shift in the resonant frequency of the antenna (≈1%) from what is predicted by the numerical code. The errors associated with the numerical code could contribute to this frequency shift. This deviation can also be attributed to the finite size of the ground plane, $0.21\lambda_0 \times 0.18\lambda_0$ for this prototype, knowing that an infinite ground plane is assumed in the numerical simulation. The shift in the resonant frequency resulted from the finite size of the ground plane for slot antennas is discussed in [15].

The far-field radiation patterns of the antenna were measured in the anechoic chamber of The University of Michigan. The gain of the antenna was measured at the bore-sight direction

TABLE V
ANTENNA CHARACTERISTICS AS A FUNCTION OF TWO DIFFERENT SIZE GROUND PLANES COMPARED WITH THE SIMULATED RESULTS FOR THE SAME ANTENNA ON AN INFINITE GROUND PLANE

Ground-Plane size $[cm]$	Resonant frequency $[MHz]$	Return Loss $[dB]$	Antenna Gain $[dB_i]$
21×18	298.1	-27	-3.0
58×43	298.8	-30	0.6
$simulation(\infty)$	300	< -30	0.75

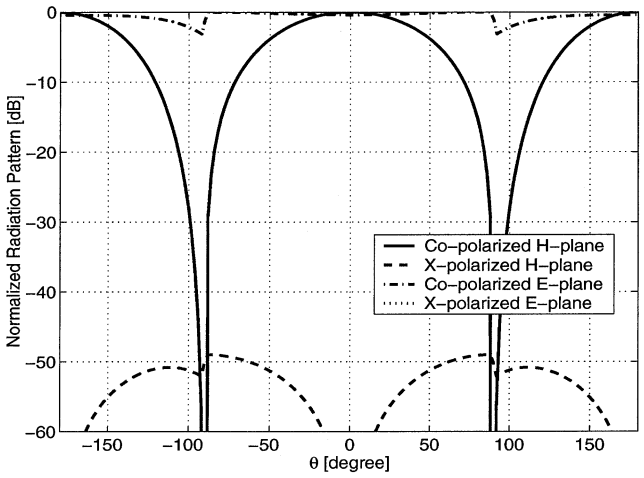

Fig. 12. Simulated radiation pattern of the miniaturized antenna.

under polarization-matched condition using a standard antenna whose gain is known as a function of frequency. The gain of -3 dBi (relative to an isotropic radiator) was measured. Having perfectly matched the impedance of the antenna, the simulated efficiency of this antenna is found to be $\eta = 87\%$ (-0.6 dB), which can exclusively be attributed to dielectric loss. Obviously, the contribution of the conductor loss, which is the main source of dissipation in slot antennas, is not accounted for in the simulated antenna efficiency. The simulated radiation efficiency is the ratio of the total radiated power to the input power of the antenna. The directivity of this antenna (with infinite ground plane) was computed to be $D = 2.0$ dB. This value of directivity is very close to that of a dipole antenna. Based on the definition of the antenna gain [16], under the impedance matched condition, one might expect to measure the maximum gain of

$$G = \eta \cdot D = -0.6\ \text{dB} + 2.0\ \text{dB} = 1.4\ \text{dB} \tag{8}$$

for this antenna. There is still a considerable difference between the measured and simulated gains (about 4.4 dB), which stems from two major factors, in addition to the ohmic loss of the ground plane. First, in the simulation, an infinite ground plane is assumed, whereas the actual ground plane size for the measured antenna is approximately $0.2\lambda_0 \times 0.2\lambda_0$. As the ground plane size decreases, the level of electric current around the edges increases considerably. This increase in the level of the electric current results in an additional ohmic loss compared to the infinite ground plane. Another reason is that as the ground plane size decreases, the directivity of the slot antenna is reduced. Basically, as the ground plane becomes smaller, the null in the pat-

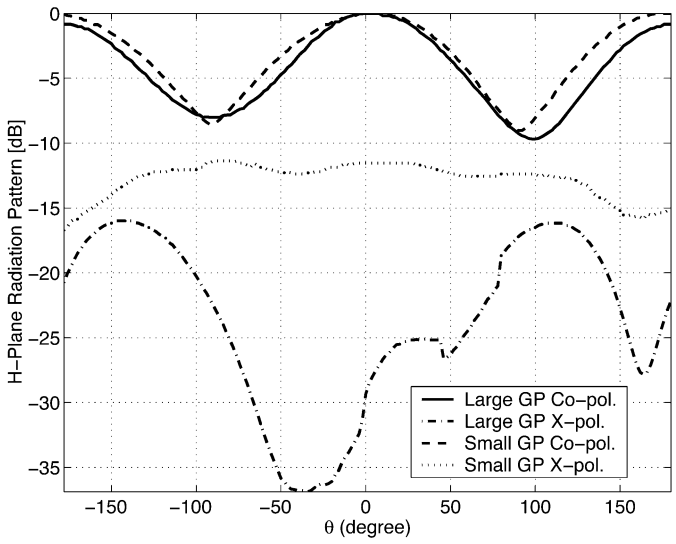

(a)

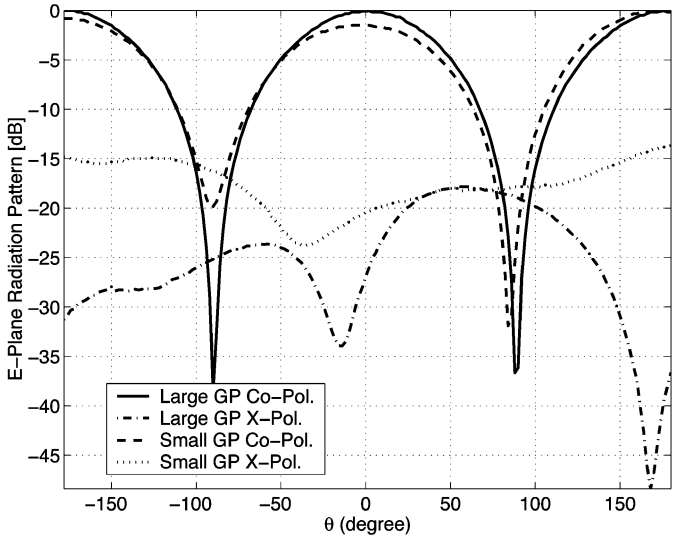

(b)

Fig. 13. Measured radiation patterns of the antenna with a small ($0.2\lambda_0 \times 0.2\lambda_0$) and a larger ($0.5\lambda_0 \times 0.5\lambda_0$) Ground Plane (GP): (a) H plane pattern. (b) E plane pattern.

tern diminishes and the pattern approaches that of an isotropic radiator. The reduction in the directivity of the slot antenna with a finite ground plane can also be attributed to the radiation from the edges and surface wave diffraction [27]. To further study the effect of the size of the ground plane, the same antenna with a slightly larger ground plane ($0.58\lambda_0 \times 0.43\lambda_0$) was fabricated and measured. Table V shows the comparison between the radiation characteristics of these two antennas and simulated results. As explained, when the size of the antenna ground plane increases, the gain of the antenna increases from -3.0 dBi to 0.6 dBi, which is almost equal to the gain of a half wavelength dipole and very close to the simulated value for the antenna gain.

Finally, the radiation patterns of the proposed antenna in the principal E and H plane were measured and compared with the theoretical ones. For H plane pattern, we measured $E_\phi(\theta)$ in the $\phi = 90°$ plane, and for E plane pattern, $E_\theta(\theta)$ was measured in the $\phi = 0°$. The simulated radiation patterns of this antenna are shown in Fig. 12. It is seen that the simulated radiation pattern of the proposed antenna with an infinite ground plane is almost the same as that of an infinitesimal slot dipole. Fig. 13(a) and (b) show the normalized co- and cross-polarized radiation patterns of the H and E plane, respectively, for two different ground planes. As expected, the null in the H plane radiation pattern is filled considerably, owing to the finite ground plane size. The ground plane enforces the tangential E-field, $E_\phi(\theta)$, to vanish along the radiating slot at $\theta = 90°$, which in fact creates the null in the H plane pattern. On the other hand, a deep null in the measured E plane pattern is observed, whereas in simulation this cut of the pattern is constant except at the dielectric-air interface where the normal E-field is discontinuous. This null in the E plane is the result of the cancellation of fields, which are radiated by the two opposing magnetic currents. The equivalent magnetic currents, flowing in the upper and lower side of the ground plane, are in opposite directions and consequently, their radiation in the point of symmetry at the E plane cancel each other. However, in the case of an infinite ground plane, the upper and lower half-spaces are isolated, and therefore, the E plane radiation pattern remains constant.

Moreover, an increase in the measured cross-polarized component is observed as compared with the simulation results. Although it may seem that there is a considerable cross-polarization radiation due to the presence of spiral slots at the terminations, there is no such component in the principal planes as well as the $\phi = \pm 45°$ planes since the geometry is symmetric with respect to those planes. The cross polarization appeared in these measurements is mainly caused by radiation from the edges as well as the feed cable. The contribution of the anechoic chamber, giving rise to the cross-polarized component at the low frequency of 300 MHz, is also a factor. The radiated field of the antenna is always capable of inducing currents on the feeding cable, especially when the ground plane size is very small compared to the wavelength. Then, the induced currents re-radiate and give rise to the cross polarization. Nevertheless, both of the above mentioned sources for the cross polarization can be eliminated by increasing the ground plane size.

VI. Conclusion

In this paper, a procedure for designing a new class of miniaturized slot antennas was proposed. In this design the area occupied by the antenna can be chosen to be arbitrarily small, depending on the applications at hand and the tradeoff between the antenna size and the required bandwidth. As an example, an antenna with the dimensions $0.05\lambda_0 \times 0.05\lambda_0$ was designed at 300 MHz and perfectly matched to a 50 Ω transmission line. In this prototype, a substrate with a low dielectric constant of $\varepsilon_r = 2.2$ was used to ensure that the dielectric material would not contribute to the antenna miniaturization. An equivalent circuit for the antenna was developed, which provided the guidelines necessary for designing a compact lossless matching network for the antenna. To validate the design procedure, a prototype antenna was fabricated and measured at 300 MHz. A perfect match for this very small antenna was demonstrated with a moderate gain of -3.0 dBi when the antenna is fabricated on a very small ground plane with the approximate dimensions of

$0.2\lambda_0 \times 0.2\lambda_0$. The gain of this antenna can increase to that of a half-wave dipole when a slightly larger ground plane of about $0.5\lambda_0 \times 0.5\lambda_0$ is used. The fractional bandwidth for this antenna was measured to be 0.034%.

REFERENCES

[1] H. A. Wheeler, "Fundamental limitations of small antennas," *Proc. IRE*, vol. 35, pp. 1479–1484, Dec. 1947.

[2] L. J. Chu, "Physical limitations of omni-directional antennas," *J. Appl. Phys.*, vol. 19, pp. 1163–1175, Dec. 1948.

[3] R. F. Harrington, "Effect of antenna size on gain, bandwidth, and efficiency," *J. Res. Natl. Bur. Stand.*, vol. 64D, pp. 1–12, 1960.

[4] H. A. Wheeler, "Small antennas," *IEEE Trans. Antennas Propagat.*, vol. AP–23, pp. 462–469, July 1975.

[5] R. E. Collin, "Small antennas," *IEEE Trans. Antennas Propagat.*, vol. AP-12, pp. 23–27, Jan. 1964.

[6] R. C. Hansen, "Fundamental limitations in antennas," *Proc IEEE*, vol. 69, pp. 170–182, Feb. 1981.

[7] J. Rashed and C. T. Tai, "A new class of Resonant antennas," *IEEE Trans. Antennas Propagat.*, vol. 39, pp. 1428–1430, Sept. 1991.

[8] J. M. Kim, J. G. Yook, W. Y. Song, Y. J. Yoon, J. Y. Park, and H. K. Park, "Compact meander-type slot antennas," in *Proc. Antennas Propagat. Soc. Int. Symp., AP-S. Dig.*, vol. 2, Boston, MA, July 2001, pp. 724–727.

[9] L. P. Ivrissimtzis, M. J. Lancaster, and M. Esa, "Miniature super conducting coplanar strip antennas for microwave and mm-wave applications," in *PROC. IEEE AP-S 9th Int. Conf. Antennas Propagat.*, vol. 1, Apr. 1995, pp. 391–395.

[10] L. P. Ivrissimtzis, M. J. Lancaster, T. S. M. Maclean, and N. McN. Alford, "High-gain series fed printed dipole arrays made of high-T superconductors," *IEEE Trans. Antennas Propagat.*, vol. 42, pp. 1419–1429, Oct. 1994.

[11] K. Noguchi, N. Yasui, M. Mizusawa, S. Betsudan, and T. Katagi, "Increasing the bandwidth of a two-strip meander-line antenna mounted on a conducting box," in *Proc. Antennas Propagat. Soc. Int. Symp., AP-S. Dig.*, vol. 4, 2001, pp. 112–115.

[12] H. Chaloupka, N. Klein, M. Peiniger, H. Piel, A. Pischke, and G. Splitt, "Miniaturized high-temperature superconductor microstrip patch antenna," *IEEE Trans. Microwave Theory Tech.*, vol. 39, pp. 1513–1521, Sept. 1991.

[13] Y.-P. Zhang, T. K.-C. Lo, and Y.-M. Hwang, "A dielectric-loaded miniature antenna for micro-cellular and personal communications," in *Antennas Propagat. Soc. Int. Symp., AP-S. Dig.*, vol. 2, 1995, pp. 1152–1155.

[14] Y. Hwang, Y. P. Zhang, K. M. Luk, and E. K. N. Yung, "Gain-enhanced miniaturised rectangular dielectric resonator antenna," *Electron. Lett.*, vol. 33, pp. 350–352, Feb. 1997.

[15] K. Sarabandi and R. Azadegan, "Design of an efficient miniaturized UHF planar antenna," in *Proc. Antennas Propagat. Soc. Int. Symp., AP-S. Dig.*, vol. 4, 2001, pp. 446–449.

[16] R. E. Collin, *Antennas and Radiowave Propagation*. New York: McGraw-Hill, 1985.

[17] B. K. Kormanyos, W. Harokopus, L. Katehi, and G. Rebeiz, "CPW-fed active slot antennas," *IEEE Trans. Microwave Theory Tech.*, vol. 42, pp. 541–545, Apr. 1994.

[18] S. Sierra-Garcia and J. Laurin, "Study of a CPW inductively coupled slot antenna," *IEEE Trans. Antennas Propagat.*, vol. 47, pp. 58–64, Jan. 1999.

[19] Roger Corporation Microwave Material Division, "RT/duroid 5880,".

[20] IE3D, "Electromagnetic Simulation and Optimization Package," Zeland Software, Inc., Fremont, CA, ver. 8.2.

[21] K. C. Gupta, P. Garg, I. Bahl, and P. Bhartia, *Microstrip Lines and Slotlines*, 2nd ed. Norwood, MA: Artec House, 1996.

[22] H. G. Akhavan and D. Mirshekar-Syahkal, "Approximate model for microstrip fed slot antennas," *Electron. Lett.*, vol. 30, pp. 1902–1903, Nov. 1994.

[23] L. Zhu and K. Wu, "Complete circuit model of microstrip-fed slot radiator: Theory and experiments," *IEEE Microwave Guided Wave Lett.*, vol. 9, pp. 305–307, Aug. 1999.

[24] M. Fariana and T. Rozzi, "A short-open deembedding technique for method-of-moments-based electromagnetic analyzes," *IEEE Trans. Microwave Theory Tech.*, vol. 49, pp. 624–628, Apr. 2001.

[25] L. Zhu and K. Wu, "Unified equivalent-circuit model of planar discontinuities suitable for field theory-based CAD and optimization of M(H)MIC's," *IEEE Trans. Microwave Theory Tech.*, vol. 47, pp. 1589–1602, Sept. 1999.

[26] J. M. Johnson and Y. Rahmat-Samii, "Genetic algorithms in engineering electromagnetics," *IEEE Antennas Propagat. Mag.*, vol. 39, pp. 7–21, Aug. 1997.

[27] B. Stockbroeckx, I. Huynen, and A. Vander Vorst, "Effect of surface wave diffraction on radiation pattern of slot antenna etched in finite ground plane," *Electron. Lett.*, vol. 36, pp. 1444–1446, Aug. 2000.

Reza Azadegan (S'98) was born in Tehran, Iran, on October 20, 1974. He received the B.S. degree from Sarif University of Technology, Tehran, Iran, and the M.S. degree, in electrical engineering, from K. N. Toosi University of Technology, Tehran, in 1996 and 1998, respectively. He is currently working toward the Ph.D. degree in the Radiation Laboratory at the University of Michigan, Ann Arbor.

From 1997 to 1999, he was with the Computational Electromagnetic Laboratory, Sharif University of Technology, as a Graduate Researcher working on the optimal design of parabolic reflector antennas using high-frequency techniques and genetic algorithms, and electromagnetic wave propagation in optical waveguides. He is working on the miniaturization of planar antennas and microwave filters for wireless communication systems.

Kamal Sarabandi (S'87–M'90–SM'92–F'00) received the B.S. degree in electrical engineering from Sharif University of Technology, Tehran, Iran, in 1980, the M.S. degree in electrical engineering in 1986, the M.S. degree in mathematics, and the Ph.D. degree in electrical engineering, all from The University of Michigan, Ann Arbor, in 1989.

He is Director of the Radiation Laboratory and a Professor with the Department of Electrical Engineering and Computer Science, University of Michigan. His research interests include microwave and millimeter-wave radar remote sensing, electromagnetic wave propagation, and antenna miniaturization. He has 20 years of experience with wave propagation in random media, communication channel modeling, microwave sensors, and radar systems and is leading a large research group, including two research scientists, ten Ph.D. and two M.S. students. Over the past ten years, he has graduated 14 Ph.D. students. He has served as the Principal Investigator on many projects sponsored by NASA, JPL, ARO, ONR, ARL, NSF, DARPA, and numerous industries. He has published many book chapters and more than 95 papers in refereed journals on electromagnetic scattering, random media modeling, wave propagation, antennas, microwave measurement techniques, radar calibration, inverse scattering problems, and microwave sensors. He also had more than 200 papers and invited presentations in many national and international conferences and symposia on similar subjects.

Dr. Sarabandi is a Vice President of the IEEE Geoscience and Remote Sensing Society (GRSS), Chairman of the Awards Committee of the IEEE GRSS, and a member of the IEEE Technical Activities Board Awards Committee. He is serving as the Associate Editor of the IEEE TRANSACTIONS ON ANTENNAS AND PROPAGATION (AP) and the IEEE *Sensors Journal*. He is a Member of Commission F of URSI and of The Electromagnetic Academy. He is listed in *American Men & Women of Science Who's Who in America* and *Who's Who in Electromagnetics*. He was the recipient of the prestigious Henry Russel Award from the Regent of The University of Michigan (the highest honor the University of Michigan bestows on a faculty member at the assistant or associate level). In 1999, he received a GAAC Distinguished Lecturer Award from the German Federal Ministry for Education, Science, and Technology given to about ten individuals worldwide in all areas of engineering, science, medicine, and law. In 1996, he received the Teaching Excellence Award from the EECS Department, The University of Michigan.